RESEARCH ARTICLE

Structural and Mechanistic Roles of Novel Chemical Ligands on the SdiA Quorum-Sensing Transcription Regulator

Y Nguyen,[a,b] Nam X. Nguyen,[c] Jamie L. Rogers,[b] Jun Liao,[c] John B. MacMillan,[b] Youxing Jiang,[c,d] Vanessa Sperandio[a,b]

Department of Microbiology, University of Texas Southwestern Medical School, Dallas, Texas, USA[a]; Department of Biochemistry, University of Texas Southwestern Medical School, Dallas, Texas, USA[b]; Department of Physiology, University of Texas Southwestern Medical School, Dallas, Texas, USA[c]; Howard Hughes Medical Institute, Dallas, Texas, USA[d]

ABSTRACT **Bacteria engage in chemical signaling, termed quorum sensing (QS), to mediate intercellular communication, mimicking multicellular organisms. The LuxR family of QS transcription factors regulates gene expression, coordinating population behavior by sensing endogenous acyl homoserine lactones (AHLs). However, some bacteria (such as *Escherichia coli*) do not produce AHLs. These LuxR orphans sense exogenous AHLs but also regulate transcription in the absence of AHLs. Importantly, this AHL-independent regulatory mechanism is still largely unknown. Here we present several structures of one such orphan LuxR-type protein, SdiA, from enterohemorrhagic *E. coli* (EHEC), in the presence and absence of AHL. SdiA is actually not in an apo state without AHL but is regulated by a previously unknown endogenous ligand, 1-octanoyl-*rac*-glycerol (OCL), which is ubiquitously found throughout the tree of life and serves as an energy source, signaling molecule, and substrate for membrane biogenesis. While exogenous AHL renders to SdiA higher stability and DNA binding affinity, OCL may function as a chemical chaperone placeholder that stabilizes SdiA, allowing for basal activity. Structural comparison between SdiA-AHL and SdiA-OCL complexes provides crucial mechanistic insights into the ligand regulation of AHL-dependent and -independent function of LuxR-type proteins. Importantly, in addition to its contribution to basic science, this work has implications for public health, inasmuch as the SdiA signaling system aids the deadly human pathogen EHEC to adapt to a commensal lifestyle in the gastrointestinal (GI) tract of cattle, its main reservoir. These studies open exciting and novel avenues to control shedding of this human pathogen in the environment.**

IMPORTANCE **Quorum sensing refers to bacterial chemical signaling. The QS acyl homoserine lactone (AHL) signals are recognized by LuxR-type receptors that regulate gene transcription. However, some bacteria have orphan LuxR-type receptors and do not produce AHLs, sensing them from other bacteria. We solved three structures of the *E. coli* SdiA orphan, in the presence and absence of AHL. SdiA with no AHL is not in an apo state but is regulated by a previously unknown endogenous ligand, 1-octanoyl-*rac*-glycerol (OCL). OCL is ubiquitously found in prokaryotes and eukaryotes and is a phospholipid precursor for membrane biogenesis and a signaling molecule. While AHL renders to SdiA higher stability and DNA-binding affinity, OCL functions as a chemical chaperone placeholder, stabilizing SdiA and allowing for basal activity. Our studies provide crucial mechanistic insights into the ligand regulation of SdiA activity.**

Received 1 December 2014 **Accepted** 10 February 2015 **Published** 31 March 2015

Citation Nguyen Y, Nguyen NX, Rogers JL, Liao J, MacMillan JB, Jiang Y, Sperandio V. 2015. Structural and mechanistic roles of novel chemical ligands on the SdiA quorum-sensing transcription regulator. mBio 6(2):e02429-14. doi:10.1128/mBio.02429-14.

Editor Edward G. Ruby, University of Wisconsin—Madison

Address correspondence to Vanessa Sperandio, vanessa.sperandio@utsouthwestern.edu, or Youxing Jiang, Youxing.Jiang@utsouthwestern.edu.

Y.N. and N.X.N. contributed equally to this article.

Chemical signaling is an effective means for cells to communicate. Chemical communication among bacterial cells occurs through quorum sensing (QS). The LuxR/I-type QS systems are commonly seen in most Gram-negative proteobacteria, where the signaling molecule is usually an endogenously produced acyl homoserine lactone (AHL). These bacteria encode both the LuxI synthase that produces the AHL signal and the cognate LuxR transcription factor, whose function is regulated by AHL (1). AHLs have a conserved homoserine lactone ring connected through an amide bond to a variable acyl chain. Acyl chains vary in length and modification of the third position, and variations in acyl chains ensure differential AHL recognition by specific LuxRs (2). Since the first discovery of the prototypical LuxR/I system in *Vibrio fischeri* (3), more than 50 species have been shown to contain LuxR/I homologs, regulating diverse biological processes (1). However, some bacteria, such as *Escherichia coli* and *Salmonella*, contain only the LuxR-type protein SdiA but not the LuxI-type synthase. While these orphan LuxR proteins can sense exogenous AHLs from other bacteria, they have also been shown to regulate gene transcription in the absence of AHLs (4–6). This observation contradicts the conventional view that AHLs are necessary for stabilizing LuxR and regulating its function and raises the possibility that the orphan LuxR sensors can detect and respond to other endogenous, non-AHL chemical signals.

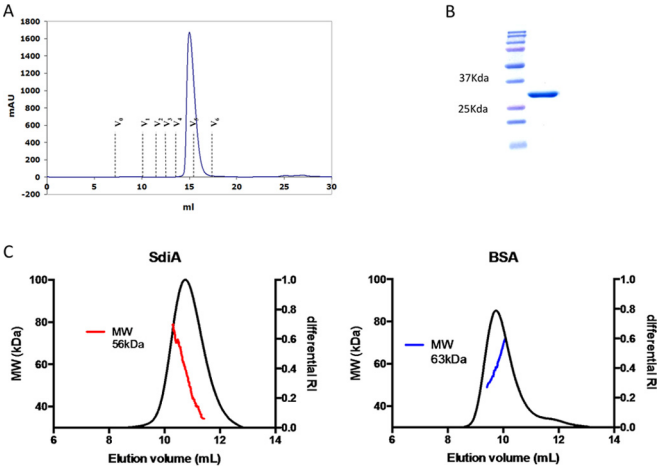

FIG 1 SdiA is soluble and a dimer without AHL. (A) Gel filtration chromatography of SdiA showing that the protein is in a dimer form (56 kDa). Samples were run on Superdex 200 10/300-Gl column. The monomer of SdiA is 28 kDa. V_0 is void volume. V_1 to V_6 are standards: V_1, apoferritin, 443 kDa; V_2, amylase, 200 kDa; V_3, alcohol dehydrogenase, 150 kDa; V_4, albumin, 66 kDa; V_5, carbonic anhydrase, 29 kDa; V_6, cytochrome *c*, 12.4 kDa. mAU, milliabsorbance units. (B) SDS-PAGE analysis of the eluted fraction. (C) SEC-MALLS measurements of SdiA and the BSA control. In the absence of AHL, SdiA is predominately dimeric (calculated molecular mass of 56 kDa). RI, refractive index.

Although extensive structural and functional studies have been performed on LuxR proteins, their AHL-dependent and -independent regulatory mechanisms remain largely unknown. It is also noteworthy that certain LuxR-type proteins are inhibited by AHLs, but the mechanism of their AHL-independent function has not been defined, and there have been no structures reported for these proteins (7). One major reason can be attributed to the instability of LuxR proteins in the absence of AHLs. To date, there are four full-length structures of the LuxR proteins (8–12) and two AHL-binding domains (13, 14) that have been solved. There is no structural information on a LuxR protein in both the absence and presence of AHL to assess the role of ligand binding in the function of these proteins.

RESULTS

Structural studies on SdiA. To reveal the structural basis of AHL-dependent and -independent function of LuxRs, we performed structural studies on the enterohemorrhagic *E. coli* (EHEC) orphan LuxR protein SdiA in the presence and absence of AHL. Previous studies suggested that AHL binding is essential for the stabilization and homodimerization of LuxR (9, 15, 16). Purified SdiA, on the other hand, forms a stable dimer in solution even in the absence of AHLs (Fig. 1). As dimerization is a requirement for LuxR family transcription factors to bind and regulate their target genes, this observation suggests that even in the absence of AHLs, SdiA is likely in a DNA-binding conformation, consistent with the observation that subsets of genes are regulated by SdiA in the absence of an AHL signal (5, 6). SdiA is known to have high sensitivity to AHL molecules with a keto modification at the third carbon and an acyl-chain length of 6 to 8 (17); we therefore crystallized SdiA in complex with two AHLs—3-oxo-C_6-homoserine lactone (HSL) and 3-oxo-C_8-HSL—as well as in the absence of AHL and determined their structures to 2.8, 2.8, and 3.1 Å, respectively.

As seen in solution, SdiA forms a dimer in the crystals both with and without AHL ligand and shares a similar overall structure that resembles that of QscR (10). Here, we use the 3-oxo-C_6-HSL–SdiA complex to describe the overall architecture of the dimer (Fig. 2A). Each subunit contains an N-terminal ligand-binding domain (LBD), which forms an α-β-α sandwich structure, and a C-terminal 4-helix DNA-binding domain (DBD), which has the classical helix-turn-helix (HTH) DNA binding motif. There are two major dimer interfaces along the 2-fold axis. The first one is between the two LBDs and involves residues mainly from the N-terminal ends of helices 1 and 8 (Fig. 2B). The other more extensive interaction is predominantly between helix 12 of each DBD (Fig. 2C, inset 1; see Fig. S1 in the supplemental material). Some residues from the LBD β-turns also participate in dimerization interactions at this interface. One particularly interesting intersubunit interaction occurs through the phenyl ring of F52 from the LBD of one subunit intercalating into a hydrophobic pocket consisting of residues from the same subunit (V50, Y233, and A236) and those from the neighboring subunit (A192, A235, and I240) (Fig. 2C, inset 2). This key-lock interaction is in a strategic position, interconnecting LBD and DBD, and could relay a conformational change at the LBD to its DBD.

SdiA DNA binding in the presence and absence of AHLs. Intriguingly, the two SdiA DBDs in both AHL-bound and -unbound states align reasonably well with each other (Fig. 3 and 4A to C), as well as with those of the DNA-bound TraR dimer, another LuxR-type protein (8, 9), indicating that the SdiA dimer adopts a similar DNA binding conformation with or without AHL. This is consistent with ours and others' reports that SdiA can bind to DNA and regulate transcription in the absence of AHLs (5, 6, 18). To examine the effect of exogenous AHL on SdiA's function, we assessed binding of SdiA on the *ler* gene in EHEC (Fig. 4D to F). The *ler* gene encodes a master transcription activator of key EHEC virulence genes, as well as the genetic repertoire EHEC utilizes to establish colonization in its natural reservoir, cattle (19, 20). SdiA-AHL has been previously shown to directly bind to and repress the transcription of this gene (5). SdiA with no AHL is able to bind to *ler* (Fig. 4D to F). However, the addition of either 3-oxo-C_6-HSL or 3-oxo-C_8-HSL increased the binding affinity of SdiA to the *ler* promoter (Fig. 4D to F; see Fig. S2). SdiA-AHL had a dissociation constant (K_d) of 16.5 μM to *ler*, while SdiA with no AHL had a K_d of 23.5 μM (Fig. 4E). This enhancement of DNA-binding affinity by AHL may allow the protein to bind and regulate transcription of certain genes, which otherwise have much lower affinity for SdiA binding. SdiA-AHL readily binds to a second site in the *ler* promoter, as evident by the supershifts of DNA probes with increasing concentration of SdiA-AHL proteins. However, SdiA with no AHL is only able to bind to one of these sites, the supershift being absent without AHL (Fig. 4D to F; see Fig. S2 in the supplemental material), suggesting that one of these sites can only be bound by the SdiA-AHL form. These data are congruent with the small structural shifts in SdiA-AHL compared to SdiA from which AHL is absent, as discussed below (Fig. 3 and 4). Although SdiA is already in a DNA-binding conformation in the absence of AHLs, AHLs enhance this protein's affinity to DNA (Fig. 4), allowing it to regulate transcription of genes that have lower-affinity sites to this protein, whose SdiA regulation occurs only in the presence of AHLs (5).

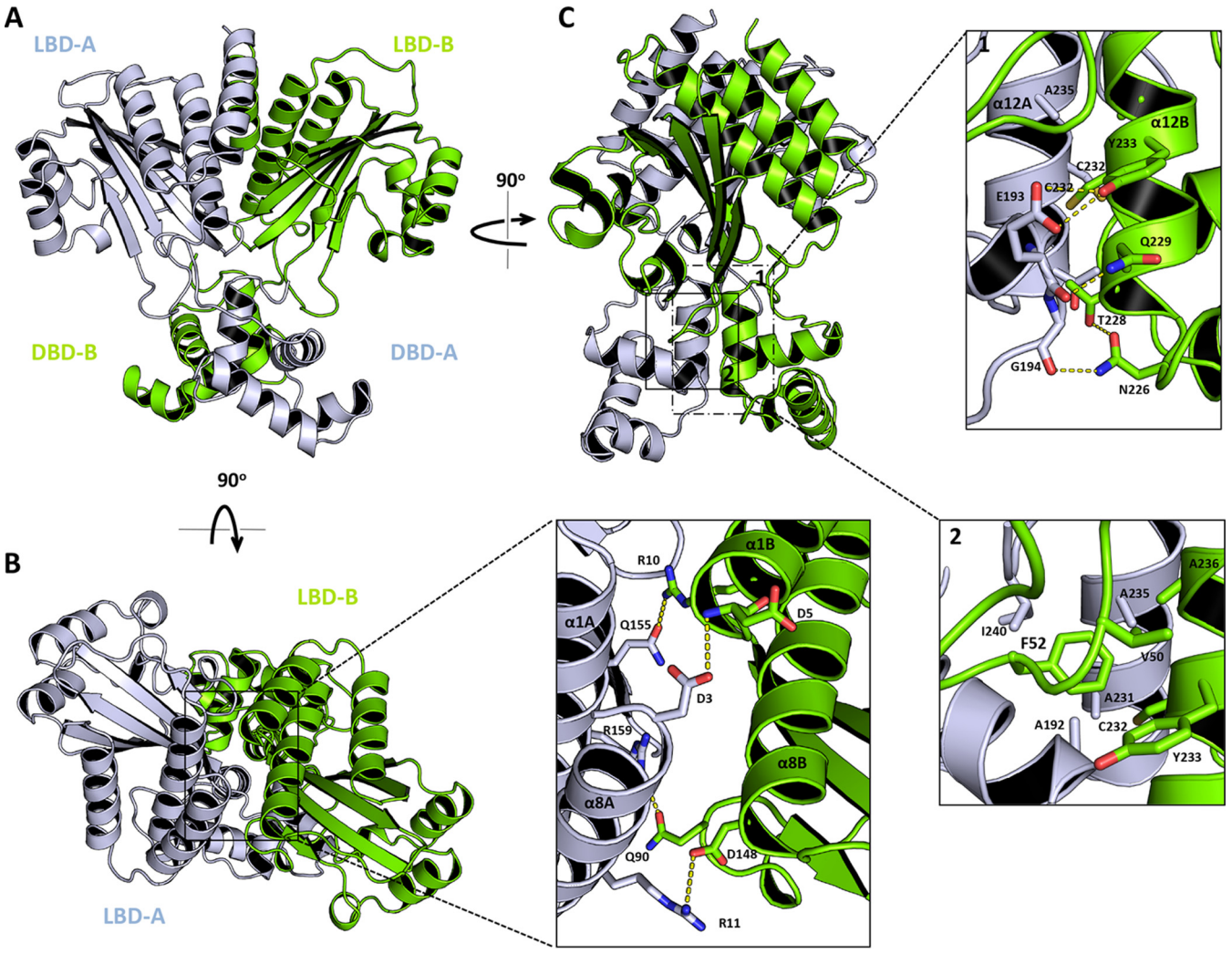

FIG 2 Analysis of the crystal structure of the SdiA dimer using SdiA−3-oxo-C_6-HSL (2.8 Å) for illustration. (A) Overall architecture of SdiA colored chartreuse and gray to represent each monomer. (B) View of the ligand-binding domain (LBD) and detailed atomic interactions (inset). (C) View of the DNA-binding domain (DBD) and atomic interactions at the DBD interface (inset 1) and the atomic interaction between the LBD and DBD (inset 2).

Consequently, how do we reconcile the observation that AHL has significant functional effects on SdiA but only introduces subtle structural changes compared to its non-AHL state? In light of the above functional data, the subtle structural change is expected given that the two HTHs have to maintain a similar relative orientation in order to straddle the major grooves of its DNA target. However, the small structural change even at a sub-Å range could be sufficient to weaken the salt bridges/H bond between protein residues and DNA bases. Indeed, the two DNA-binding HTHs do show sub-Å conformational change upon AHL binding (Fig. 4A to C).

AHLs enhance SdiA protein stability. In addition to increasing DNA binding affinity, AHLs can significantly stabilize SdiA and prolong its lifetime *in vivo*, as was demonstrated in the following two experiments. First, we chromosomally FLAG-tagged SdiA in wild-type (WT) EHEC and measured endogenous levels of SdiA in the absence (in dimethyl sulfoxide [DMSO] solvent) or presence of increasing concentrations of AHLs (diluted in DMSO). In the absence of exogenous AHLs, only a small amount of SdiA is detected, but the amount is significantly increased when AHLs are present (Fig. 5A). AHLs regulate SdiA posttranscriptionally, as an increase in SdiA protein levels (see Fig. S3 in the supplemental material) does not correspond to an increase in *sdiA* mRNA, which is not affected by AHLs (see Fig. S3). Second, the pulse-chase experiments on SdiA in the presence or absence of AHLs demonstrated that the increased SdiA levels are the result of enhanced stabilization of SdiA by AHLs (Fig. 5B and C), hence decreasing the rate of protein degradation. The DNA binding and protein stability data suggest a double mode of action for AHLs on SdiA activity, by increasing both protein stability and DNA binding.

Differences in the SdiA LBD in the presence and absence of AHL. In addition to the subtle conformational change at the DBD between the structures with AHL and those without it, careful structural analysis also reveals two novel findings at the LBD. First, there are noticeable structural differences at the ligand binding sites between AHL-bound and -unbound states (Fig. 5D to G). AHL binding in SdiA is similar to that of other AHL-bound LuxR

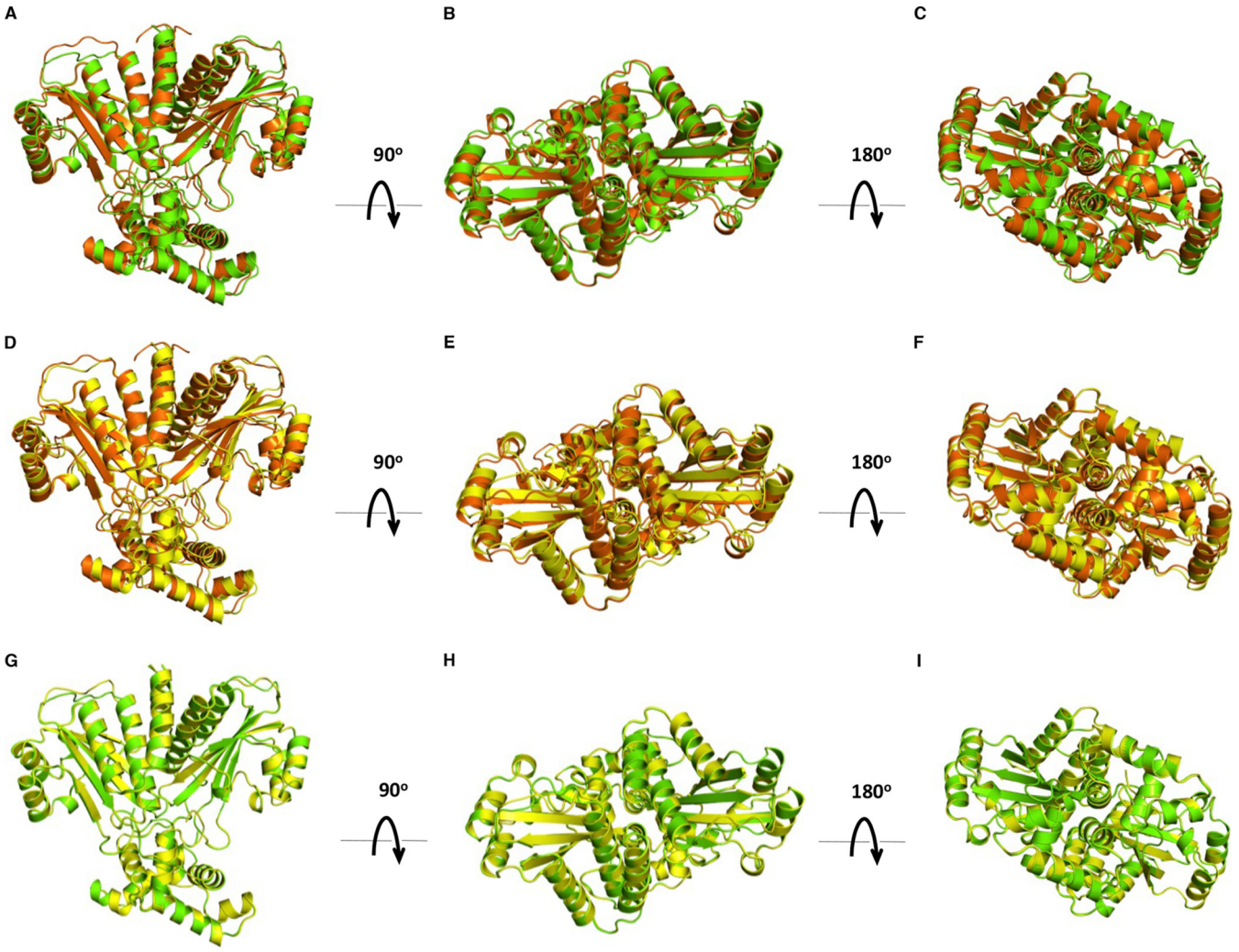

FIG 3 Structural alignment between SdiA dimers without AHL (orange) and with 3-oxo-C_6-HSL (chartreuse) (A), 3-oxo-C_8-HSL (yellow) (D), or 3-oxo-C_6-HSL and 3-oxo-C_8-HSL (G). Panels A, D, and G show full-length structural alignment. Panels B, E, and H show views from the ligand binding domain, and panels C, F, and I show views from the nucleotide binding domain.

proteins (8, 9), with the lactone ring forming specific AHL H-bond interactions with several highly conserved residues and the acyl chain being stabilized by hydrophobic residues. Specifically H bonds are formed between W67 and the lactone ring, Y63 and the carbonyl on C1, D80 and amine, and S43 and carbonyl on C3. The mono-acyl chain of AHL packs within the cavity through hydrophobic interactions with F59, T61, Y63, Y71, and L77 (Fig. 5E). The SdiA proteins complexed with oxo-C_6-HSL or oxo-C_8-HSL align perfectly with each other, suggesting that both signals yield proteins in similar conformation (Fig. 3; see Fig. S4 in the supplemental material). The bound AHL is occluded from solvent access, making the protein-AHL complex a tightly packed entity (Fig. 5D). In the AHL-unbound state, on the other hand, the ligand-binding pocket becomes an open chamber that traverses the LBD with solvent exposure on both ends (Fig. 5F; see Fig. S4). Compared to the AHL-bound state, this open chamber formation in the absence of AHL results mainly from side-chain movement of three residues—F59, L77, and W107 (Fig. 5G). In going from the AHL-unbound state to the AHL-bound state, L77 descends by 3.6 Å and F59 tilts by 1.6 Å, respectively, toward the acyl chain of AHL to occlude one end of the ligand-binding pocket, while W107 undergoes nearly a 147° flip into the ligand-binding pocket to cap off the other end of the cavity (Fig. 5G). Binding of oxo-C_6-HSL and oxo-C_8-HSL to the LDB is generally conserved, and the H bond of Y63 with the C_3 keto group is clearly important for specific and high-affinity binding. The length of the acyl chain that can be accommodated in the hydrophobic pocket seems to be limited by the hydrophobic residues F59 and L77 (Fig. 5E). A longer acyl chain would clash with these residues based on the structure of the LBD.

SdiA has an endogenous ligand. The second intriguing finding is that the ligand-binding pocket in the AHL-unbound state is actually not empty or filled with solvent. The structure of SdiA without AHL clearly shows multiple discrete electron density peaks, termed sites P1 to P3 from one end to the other, indicating the binding of several non-AHL ligands, which have to come from the *E. coli* cell used for protein expression (Fig. 5F). To identify this unknown mass, the ligand was extracted from purified SdiA with ethyl acetate, purified using high-performance liquid chromatography (HPLC), and subjected to nuclear magnetic resonance

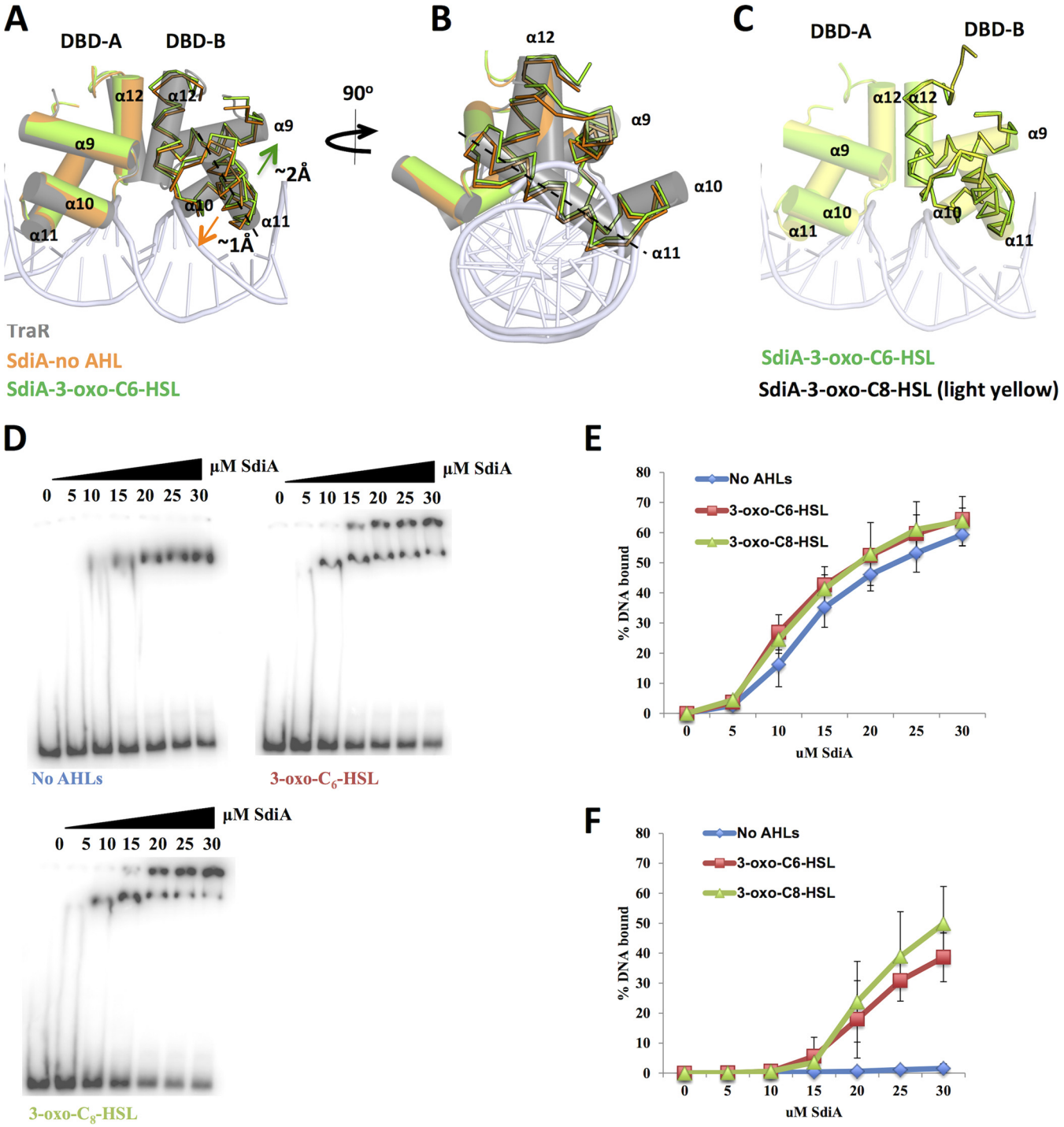

FIG 4 AHLs increase SdiA DNA-binding affinity and stability. (A) The DBDs of SdiA with no AHL (orange cylinders and ribbon) and SdiA−3-oxo-C_6-HSL (chartreuse cylinders and ribbon) are aligned to the DBD of TraR (gray cylinders) and its cocrystallized DNA. Helices α10 and α11 form the HTH motif on SdiA involved in DNA binding, with α11 positioned in the major groove of the modeled DNA. Relative to the DBD of TraR, the DBD of SdiA-OCL moves down toward the major groove of DNA by ~1 Å, whereas the DBD of SdiA−3-oxo-C_6-HSL tilts up toward α9 by ~2 Å. (B) View of the DBD of TraR and SdiA through the vertical axis of the modeled DNA. (C) The DBDs of SdiA–3-oxo-C_6-HSL (chartreuse cylinders and ribbon) and SdiA–3-oxo-C_8-HSL (yellow cylinders and ribbon) are aligned to the DBD of TraR (not shown) and its cocrystallized DNA. (D) Electrophoretic mobility shift assays to determine the binding affinities of SdiA in the absence or presence of AHLs. The same DNA fragment as in panel E was incubated with increasing concentrations of SdiA (0 to 30 μM) in the absence or presence of 10 μM exogenous 3-oxo-C_6-HSL or 3-oxo-C_8-HSL, and binding affinities (K_ds) were calculated in panel E. (F) Measurement of the supershift band from SdiA EMSAs in the absence and presence of AHLs.

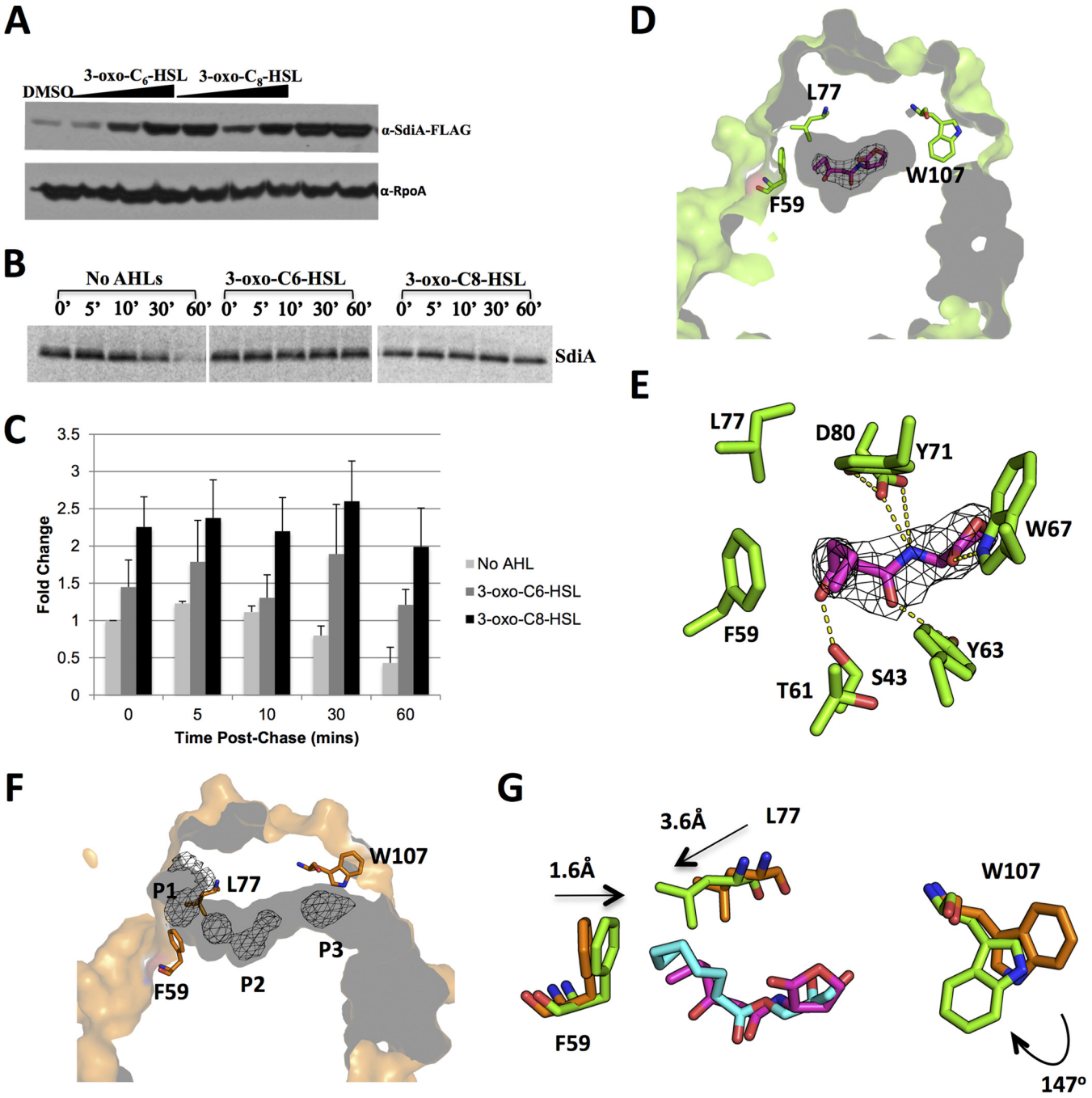

FIG 5 AHL's role in SdiA stability. (A) Western blot of whole-cell lysates of wild-type EHEC with chromosomally FLAG-tagged SdiA grown in DMEM supplemented with either increasing concentrations of exogenous AHLs 3-oxo-C_6-HSL and 3-oxo-C_8-HSL or equivalent amounts of DMSO as the no-AHL control to the late log phase. RpoA was used as a loading control. (B) Wild-type EHEC cells expressing SdiA from a phage T7 promoter were treated with rifampin to block host transcription, followed by [^{35}S]methionine and excess nonlabeled methionine 10 min later to inhibit labeling. AHLs or DMSO was added 30 min before the addition of the radiolabel. Samples were collected at 0, 5, 10, 30, and 60 min after the addition of the nonlabeled methionine. Radioactivity of soluble SdiA was quantified using the Storm PhosphorImager (C). (D) The bound 3-oxo-C_6-HSL ($2F_o$-F_c electron density map, black mesh, contoured at 1σ) makes the protein-AHL complex a tightly packed entity. (E) The 3-oxo-C_6-HSL forms four hydrogen bonds directly with surrounding residues, as indicated by the dashed lines. (F) In the absence of AHL, the pocket adopts an open conformation that is solvent accessible and traverses the entire length of the cavity. The F_o-F_c map (black mesh), contoured at 3.5σ, shows three distinct electron densities (labeled P1 to P3) occupying the ligand-binding cavity. (G) Three residues contribute to the transition from an open (orange) to occluded (chartreuse) cavity. L77 descends by 3.6 Å and F59 tilts by 1.6 Å, respectively, toward the acyl chain of AHL to occlude one end of the ligand-binding pocket, while W107 undergoes nearly a 147° flip into the ligand-binding pocket to cap off the other end of the cavity.

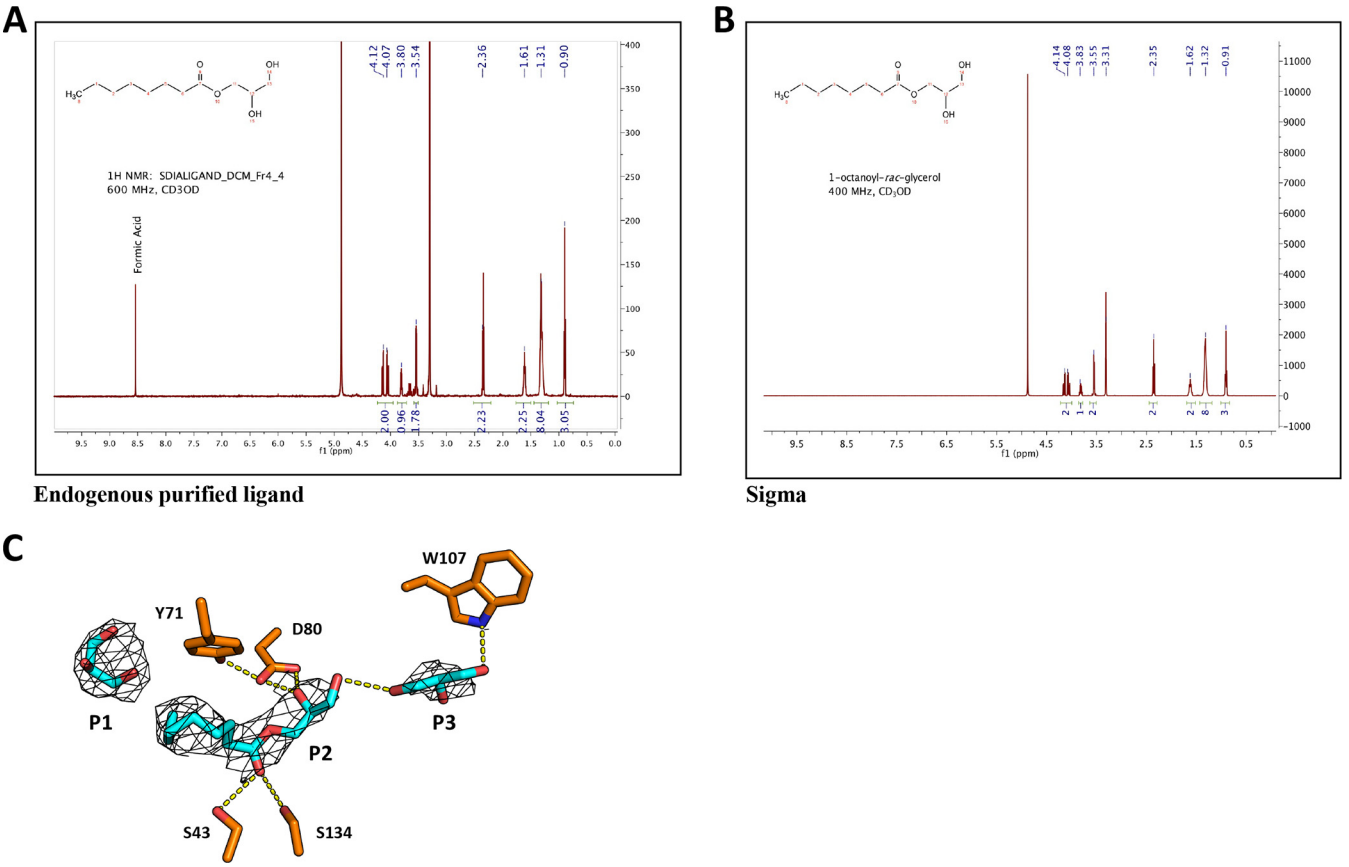

FIG 6 *E. coli* produces an endogenous ligand 1-octanoyl-*rac*-glycerol that binds to SdiA in the absence of AHL. This endogenous ligand was purified, identified, and confirmed by NMR to be 1-octanoyl-*rac*-glycerol from ligand purified from SdiA, the peak at 3.30 ppm identification no. CD3OD that is the solvent used for the NMR (A) and a commercial (Sigma) source (B). (C) Close-up view of the ligand-binding pocket with 1-octanoyl-*rac*-glycerol modeled into the electron density ($2F_o$-F_c map contoured at 1σ, black mesh). The 1-octanoyl-*rac*-glycerol and the two glycerol molecules (cyan) form several hydrogen bonds with surrounding residues, as indicated by the dashed lines.

(NMR) analysis. The extracted ligand was identified (Fig. 6A) and confirmed (Fig. 6B) to be 1-octanoyl-*rac*-glycerol (OCL). Upon the identification of the endogenous ligand, we could fit one OCL molecule into the P2 density at the center of the open chamber (Fig. 6C). The P1 and P3 density peaks at the two ends of the chamber were modeled as two glycerol molecules. We believe these glycerol molecules could come from the glycerol moieties of the OCL ligands whose acyl chains are disordered. P2 OCL overlaps with the AHL binding site (Fig. 5F and G) and forms H bonds with D80, S43, and S134: these residues are reasonably conserved within LuxR-type proteins, and D80 and S43 also form hydrogen bonds with AHLs in SdiA-AHL (Fig. 5E and 6C; see Fig. S1 in the supplemental material); P2 OCL appears to have higher occupancy than OCLs at P1 and P3, which could be attributed to the partial loss of OCL ligands during the purification and crystallization process. A previous report of a crystal structure of SdiA without AHL also found a density within the LBD. The authors modeled four tetraethylene glycol (TEG molecules) in the LBD but did not really explore the nature of this density (12). We believe that TEG cannot be a potential ligand for the electron density in the ligand-binding pocket of our SdiA-no AHL structure. First, alignment of the SdiA-OCL and SdiA-TEG (PDB no. 4LFU) structures shows that α7 and β4 have to undergo significant movement in order for SdiA to accommodate the two TEG molecules seen in the structure shown by Kim et al. in reference 12. Additionally, the alignment shows that OCL and TEG molecules occupy very different binding sites in the two SdiA structures; in fact, OCL is oriented nearly perpendicular to the TEG molecules (see Fig. S5 in the supplemental material). Second, we modeled the TEG molecule into the electron density identified in our omit map of SdiA with no AHL, and TEG does not fit into this density. Given these observations and the results of our ligand identification experiments, we are confident that TEG is not a ligand in our SdiA structure and that OCL is the bona fide endogenous ligand.

DISCUSSION

In summary, the structural studies of SdiA provide insights into the AHL regulation of LuxR proteins. The endogenous ligand and the open transverse ligand-binding cavity adopted by SdiA in the absence of AHL suggest that SdiA, and potentially other LuxRs, detects non-AHL signals, allowing bacterial adaptation to different environments. It is noteworthy that other LuxR orphans have been reported to detect non-AHL signals (21, 22). In a broader sense, the discovery of a monoacylglycerol as an SdiA ligand breaks new ground in the understanding of LuxR-type proteins. Several LuxR-type proteins have their DNA binding properties inhibited by AHLs (7, 23), and it has been largely assumed that these LuxRs are apoproteins, when in fact they may be complexed

with monoacylglycerols, and this could be a "molecular chaperone placeholder" for many LuxRs in the absence of AHLs. OCL is a monoacylglycerol, which are the building blocks of triacylglycerols and are present in both eukaryotes and prokaryotes (24). Monoacylglycerols are highly abundant in the mammalian gastrointestinal (GI) tract and serve as energy sources, signaling molecules, and substrates for membrane biogenesis (25). Since *E. coli* and *Salmonella* colonize the gut, these bacteria utilize SdiA to detect self, microbiota, or host-derived monoacylglycerols to promote colonization in various eukaryotic hosts (5, 26). Thus far, monoacylclygerols have only been implicated in membrane biogenesis in prokaryotes, and here we show that these molecules can also be used as a chemical chaperone for a protein. Moreover, monoacylglycerols are highly prevalent in the mammalian intestine, suggesting that SdiA-OCL may have AHL-independent functions that are relevant to virulence of intestinal pathogens.

MATERIALS AND METHODS

Strains and plasmids. All strains and plasmids used in this study are listed in Table S1 in the supplemental material. Unless otherwise stated, *E. coli* strains were grown aerobically in Luria-Bertani (LB) broth at 37°C and 250 rpm. Where indicated, strains were grown in low-glucose Dulbecco's modified Eagle's medium (DMEM) (Invitrogen). Antibiotics were added at the following final concentrations: 100 μg/ml streptomycin, 50 μg/ml kanamycin, and 100 μg/ml ampicillin.

Recombinant DNA techniques. The methods for PCR amplification, plasmid purification, and transformations were performed using standard protocols as previously described (27). Oligonucleotide primers (see Table S1 in the supplemental material) were designed by using Primer Express v1.5 (Applied Biosystems). The wild-type EHEC strain expressing chromosomally 3× FLAG-tagged SdiA was constructed using recombinant DNA techniques as described previously in references 28 and 29. Briefly, PCR product was amplified using Phusion high-fidelity DNA polymerase (Thermo Scientific), sdiAFLAGF and sdiAFLAGR primers, and pSUB11 (Kn^r) plasmid as the template. PCR product was digested with DpnI to remove the template DNA and then gel purified (Qiagen). Cells of the wild-type EHEC strain transformed with the helper plasmid pKD46 were prepared for electroporation and transformed with the resulting gel-purified PCR products. Colonies were screened for ampicillin sensitivity and kanamycin resistance. Successful recombinational transfer of the FLAG sequence into the chromosomal *sdiA* gene of positive colonies was confirmed by PCR amplification of the integrated region using primers sdiAUP and sdiADOWN. The kanamycin cassette was removed with the resolvase plasmid pCP20. PCR amplification and DNA sequencing were performed for final verification of the resolved chromosomal 3× FLAG-tagged SdiA EHEC strain, YNN04.

SdiA vector construction, expression, and protein purification. The plasmid pYN1 was constructed by PCR amplification of the *sdiA* gene from the 86-24 genome using Phusion high-fidelity DNA polymerase (Thermo Scientific) with the primers SdiAF-pET21 and SdiAR-pET21 and cloning the resulting PCR product into the EcoRI and SalI cloning sites of the pET-21a expression vector. The resulting plasmid, pYN2, was transformed into BL21 cells. Transformed BL21 cells were cultured in LB broth with 100 μg/ml of ampicillin to an optical density at 600 nm (OD_{600}) of 0.8 at 37°C and were induced with 400 μM isopropyl-β-D-1-thiogalactopyranoside (IPTG) (Sigma) at 15°C overnight. Cells were harvested, suspended in lysis buffer (50 mM Tris-base buffer [pH 8.5], 300 mM NaCl, 1 mM EDTA, 5 mM imidazole, 5 mM 2-β-mercaptoethanol, 5% glycerol), and lysed by homogenization. The lysed cells were centrifuged, and the lysates were incubated with Ni^{2+}-nitrilotriacetic acid (NTA) agarose beads (Qiagen) and loaded onto a gravity column (Qiagen). The column was washed with wash buffer 1 (50 mM Tris-base buffer [pH 8.5], 300 mM NaCl, 0.1 mM EDTA, 10 mM imidazole, 5 mM 2-β-mercaptoethanol, 5% glycerol) and wash buffer 2 (50 mM Tris-base buffer [pH 8.5], 300 mM NaCl, 0.1 mM EDTA, 50 mM imidazole, 5 mM 2-β-mercaptoethanol, 5% glycerol), and the protein was eluted in the elution buffer (50 mM Tris-base buffer [pH 8.5], 300 mM NaCl, 0.1 mM EDTA, 250 mM imidazole, 5 mM 2-β-mercaptoethanol, 10% glycerol). SdiA was concentrated for further use.

EMSAs. To assess the effects of AHLs on SdiA binding to the *ler* promoter, electrophoretic mobility shift assays (EMSAs) were performed with purified SdiA in the presence or absence of 3-oxo-C_6-HSL or 3-oxo-C_8-HSL and labeled *ler* DNA probe. The *ler* probe was defined as +86 bp downstream and −218 bp upstream from the P2 start site. The promoter region was amplified from the 86-24 genome using primers R2 and Ler-218F and Phusion high-fidelity DNA polymerase (Thermo Scientific). The *kan* promoter region, used as a negative control, was amplified from the pRS551 plasmid with primers KanF and KanR. The resulting PCR products were gel extracted (Qiagen) and end labeled with [^{32}P]ATP (PerkinElmer) using T4 polynucleotide kinases (NEB) and standard procedures (27). The end-labeled DNA fragments were purified using the Qiagen PCR purification kit. EMSAs were performed by adding increasing amounts of purified SdiA protein (0 to 30 μM) to end-labeled probes in binding buffer [50 mM Tris-HCl (pH 8.5), 50 mM NaCl, 2-mM magnesium acetate, 0.1 M EDTA, 0.1 mM dithiothreitol (DTT), 25 μg/ml bovine serum albumin (BSA), 1 μg of poly(dI-dC)] with 2× the concentration of oxo-C_6-HSL or oxo-C_8-HSL for SdiA or corresponding amounts of DMSO as a solvent control for 20 min at 22°C. Immediately before loading, a 5% Ficoll solution was added to the mixtures. The reaction mixtures were electrophoresed for ~6 h at 160 V on a 5% polyacrylamide gel, dried, exposed, and analyzed using the Storm PhosphorImager.

Pulse-chase experiments. To measure the stability of SdiA *in vivo*, pYN1 (which expresses SdiA protein) and pJD410 (which expresses T7 RNA polymerase) (16) were transformed into wild-type EHEC 86-24, and the resulting strain, YNN05, was used for the pulse-chase experiments. YNN05 was cultured in M9 minimal medium containing 100 μg/ml of ampicillin at 37°C to an OD_{600} of 0.7 and then switched to 45°C for 20 min to induce T7 RNA polymerase expression. The temperature was changed back to 37°C, and SdiA protein expression was induced with 400 μM IPTG for 20 min in either the presence of AHLs by adding 10 μM 3-oxo-C_6-HSL or 10 μM 3-oxo-C_8-HSL or in the absence of AHLs by adding the equivalent amount of DMSO. Cells were treated with a final concentration of 200 μg/ml rifampin to inhibit the host RNA polymerase for 10 min and then labeled with [^{35}S]methionine at a final concentration of 5 μCi/ml. After 10 min, 5 mM nonlabeled methionine was added to stop incorporation of the radiolabeled amino acid, and 10 ml of the culture was collected at 0, 5, 10, 30, and 60 min postaddition of the cold methionine. Samples were centrifuged and lysed with 250 μl of lysis buffer (50 mM Tris-base buffer [pH 8.5], 300 mM NaCl, 1 mM EDTA, 5 mM imidazole, 5 mM 2-β-mercaptoethanol, 5% glycerol, 1 mg/ml lysozyme, 0.1 mg/ml phenylmethylsulfonyl fluoride [PMSF]) for 1 h at 4°C. Cell lysates were collected by centrifugation (13,000 × g for 30 min), and 30 μl of the samples was electrophoresed in sodium dodecyl sulfate–12% polyacrylamide gels and analyzed using the Storm PhosphorImager.

Western blotting. To access how AHLs affect endogenous levels of SdiA protein, overnight cultures of YNN04 grown aerobically at 37°C in LB were diluted at 1:100 into low-glucose DMEM in the presence or absence of 10 μM oxo-C_6-HSL or 10 μM oxo-C_8-HSL. At the late log growth phase (OD_{600} of 1.0), cells were collected by centrifugation and lysed at room temperature in urea lysis buffer (100 mM NaH_2PO_4, 10 mM Tris-Cl, 8 M urea [pH 8.0]) for 2 h. Cellular debris was removed by centrifugation, and whole-cell lysates were electrophoresed in sodium dodecyl sulfate–12% polyacrylamide gels by SDS-PAGE. Samples were subjected to immunoblotting as described previously (27). Blots were probed with a mouse monoclonal antibody to FLAG (Sigma) (1:5,000) and RpoA (Santa Cruz) (1:5,000) and visualized by enhanced chemiluminescence (GE Healthcare).

RNA extraction. Overnight cultures of YNN04 grown aerobically at 37°C in LB were diluted at 1:100 into low-glucose DMEM and grown in triplicate to the early (OD_{600} of 0.1), mid (OD_{600} of 0.5)-, and late (OD_{600}

of 1.0) exponential growth phases in the absence or presence of 10 μM oxo-C_6-HSL. For samples assessed without exogenous signals, the respective concentration of DMSO was used to ensure that the solvent did not alter gene expression. Samples were split for Western blotting as described above and for RNA extraction using TRIzol (Invitrogen) and the RiboPure bacterial RNA isolation kit (Ambion) according to the manufacturer's instructions.

Real-time qRT-PCR. The primers sdiARTF and sdiARTR used for the real-time PCR assays were designed by using Primer Express v1.5 (Applied Biosystems) (see Table S1 in the supplemental material). Primer validation and reaction mixture preparation were done as previously described (30). Quantitative real-time reverse transcriptase PCR (qRT-PCR) was performed in a one-step reaction using the ABI 7500 sequence detection system (Applied Biosystems). Using the ABI sequence detection 1.2 software (Applied Biosystems), data were collected and normalized to endogenous levels of *rpoA*. Data were analyzed by using the comparative critical threshold cycle (C_T) method and are presented as fold changes compared to levels of the WT strain grown to the early log growth phase without AHLs. Error bars represent the standard deviations of the C_T values.

SEC-MALLS experiment. To determine the absolute molecular weight of SdiA purified in the absence of AHL, the size exclusion chromatography-multiangle laser light scattering (SEC-MALLS) experiment was performed using the mini-DAWN Treos static light scattering instrument (Wyatt) equipped with an in-line refractive index detector. The full length of SdiA was expressed and purified as described above. A 400-μl sample containing 60 μM SdiA was injected onto a Superdex 75 (10/300) analytical gel filtration column to separate oligomeric species and protein aggregates. Molecular mass determinations were subsequently determined via in-line MALLS detection and calculated using Wyatt Astra software.

Structure determination of SdiA. Full-length SdiA was expressed, purified, and crystallized in the absence of AHL. As judged by its elution volume on gel filtration chromatography, SdiA exists as a dimer in solution. Although SdiA can be purified at typical protein concentrations for crystallization, the best crystals of SdiA were obtained by the hanging-drop vapor diffusion method on SdiA (1.0 to 1.5 mg/ml) at 4°C; initial crystals appeared within 2 to 3 days and grew to their full size in about 2 weeks. These crystals consistently diffract X rays between 3.5 and 3.1 Å using synchrotron radiation and belonged to space group $P6_522$. The experimental phase was obtained by SAD (single-wavelength anomalous dispersion) phasing using crystals of seleno-methionine-derived SdiA. To obtain the SdiA-AHL complex, purified protein was incubated with 5 mM either 3-oxo-C_6-HSL or 3-oxo-C_8-HSL for 1 h on ice prior to crystallization. These crystals diffracted X-rays to 2.8 Å and belonged to space group $P2_12_12$. The SdiA-AHL complex was determined by molecular replacement using the AHL-free SdiA structure as the search model. Diffraction data were processed using HKL2000, and the structures were built in Coot and refined in PHENIX: statistics for these structures are summarized in Table S2 in the supplemental material. The SdiA crystal without AHL contains only 1 subunit per asymmetric unit, and therefore its molecular dyad coincides with a crystallographic 2-fold symmetry. The SdiA-AHL complexes contain three subunits in an asymmetric unit with one of the subunits forming a dimer with its crystallographic symmetry-related partner.

Endogenous ligand extraction and identification. SdiA was purified from 6-liter cultures of YNN07 as described above and eluted in 300 ml of elution buffer. Endogenous ligand was extracted from the purified SdiA three times with ethyl acetate at 1:1 vol/vol ratio. The combined organic phase was concentrated under reduced pressure. The residue was then partitioned between H_2O and *n*-hexane. The aqueous phase was further extracted sequentially with $CHCl3_3$ and 1-butanol. The $CHCl_3$ soluble portion was further purified via reversed-phase HPLC (Phenomenex, C_{18}, 250 by 10.0 mm, 2.5 ml/min, 5 mm, UV at 240 nm) using a gradient solvent system from 10% CH_3CN to 100% CH_3CN (0.1% fluorescent antibody [FA]) over 40 min. Eight fractions were collected across 5-min time intervals. Fraction 4 was further purified via reversed-phase HPLC (same column as before) with a gradient solvent system from 20% CH_3CN to 75% CH_3CN (0.1% FA) over 30 min to afford (2,3)dihydroxypropyl octanoate as a colorless residue.

The analytical data are as follows: ^{1}H NMR (600 MHz, CD_3OD), d 4.12 (dd, J = 11.4, 4.3 Hz, 1H), 4.07 (dd, J = 11.4, 4.3 Hz, 1H), 3.79 (m, 1H), 3.53 (dd, J = 2.9, 2.5 Hz, 1H), 2.32 (t, J = 7.4 Hz, 2H), 1.58 (m, 2H), 1.27 (m, 8H), 0.87 (t, J = 6.9 Hz, 3H); ^{13}C NMR (125 MHz, CD_3OD), d 174.0, 71.2, 66.2, 64.0, 36.2, 34.9, 28.5, 28.1, 25.7, 23.6, 14.4.

Macromolecular structure deposition numbers. The atomic coordinates and structural factors have been deposited in the Protein Data Bank with the accession numbers 4Y13 (for SdiA no AHL), 4Y15 (for SdiA in complex with 3-oxo-C_6-HSL), and 4Y17 (for SdiA in complex with 3-oxo-C_8-HSL).

SUPPLEMENTAL MATERIAL

Supplemental material for this article may be found at http://mbio.asm.org/lookup/suppl/doi:10.1128/mBio.02429-14/-/DCSupplemental.

Figure S1, PDF file, 0.2 MB.
Figure S2, PDF file, 0.3 MB.
Figure S3, PDF file, 0.1 MB.
Figure S4, PDF file, 0.1 MB.
Figure S5, PDF file, 0.1 MB.
Table S1, PDF file, 0.05 MB.
Table S2, PDF file, 0.02 MB.

ACKNOWLEDGMENTS

This work was supported by NIH grant AI077613 and the Burroughs Wellcome Fund. Y.J. is an HHMI investigator.

Structures shown in this report are derived from work performed at the Advanced Photon Source (23-ID beamlines), Argonne National Laboratory. Use of the Advanced Photon Source, an Office of Science User Facility operated for the U.S. Department of Energy (DOE) Office of Science by Argonne National Laboratory, was supported by the U.S. DOE under contract no. DE-AC02-06CH11357. We thank the beamline staff for assistance in data collection.

We thank J. Zhu at the University of Pennsylvania for constructs to perform the pulse-chase experiments. We thank Victor Ocasio and Kevin Gardner at University of Texas Southwestern for helping with the SEC-MALLS measurements of SdiA.

REFERENCES

1. **Schuster M, Sexton DJ, Diggle SP, Greenberg EP**. 2013. Acyl-homoserine lactone quorum sensing: from evolution to application. Annu Rev Microbiol **67:**43–63. http://dx.doi.org/10.1146/annurev-micro-092412-155635.
2. **Fuqua C, Greenberg EP**. 2002. Listening in on bacteria: acyl-homoserine lactone signalling. Nat Rev Mol Cell Biol **3:**685–695. http://dx.doi.org/10.1038/nrm907.
3. **Nealson KH, Platt T, Hastings JW**. 1970. Cellular control of the synthesis and activity of the bacterial luminescent system. J Bacteriol **104:**313–322.
4. **Lee JH, Lequette Y, Greenberg EP**. 2006. Activity of purified QscR, a *Pseudomonas aeruginosa* orphan quorum-sensing transcription factor. Mol Microbiol **59:**602–609. http://dx.doi.org/10.1111/j.1365-2958.2005.04960.x.
5. **Hughes DT, Terekhova DA, Liou L, Hovde CJ, Sahl JW, Patankar AV, Gonzalez JE, Edrington TS, Rasko DA, Sperandio V**. 2010. Chemical sensing in mammalian host-bacterial commensal associations. Proc Natl Acad Sci U S A **107:**9831–9836. http://dx.doi.org/10.1073/pnas.1002551107.
6. **Dyszel JL, Soares JA, Swearingen MC, Lindsay A, Smith JN, Ahmer BM**. 2010. *E. coli* K-12 and EHEC genes regulated by SdiA. PLoS One **5:**e8946. http://dx.doi.org/10.1371/journal.pone.0008946.
7. **Ryan GT, Wei Y, Winans SC**. 2013. A LuxR-type repressor of *Burkholderia cenocepacia* inhibits transcription via antiactivation and is inactivated by its cognate acylhomoserine lactone. Mol Microbiol **87:**94–111. http://dx.doi.org/10.1111/mmi.12085.
8. **Vannini A, Volpari C, Gargioli C, Muraglia E, Cortese R, De Francesco**

R, Neddermann P, Marco SD. 2002. The crystal structure of the quorum sensing protein TraR bound to its autoinducer and target DNA. EMBO J **21:**4393–4401. http://dx.doi.org/10.1093/emboj/cdf459.

9. **Zhang RG, Pappas KM, Brace JL, Miller PC, Oulmassov T, Molyneaux JM, Anderson JC, Bashkin JK, Winans SC, Joachimiak A.** 2002. Structure of a bacterial quorum-sensing transcription factor complexed with pheromone and DNA. Nature **417:**971–974. http://dx.doi.org/10.1038/nature00833.
10. **Lintz MJ, Oinuma K, Wysoczynski CL, Greenberg EP, Churchill ME.** 2011. Crystal structure of QscR, a *Pseudomonas aeruginosa* quorum sensing signal receptor. Proc Natl Acad Sci U S A **108:**-15763–15768. http://dx.doi.org/10.1073/pnas.1112398108.
11. **Chen G, Swem LR, Swem DL, Stauff DL, O'Loughlin CT, Jeffrey PD, Bassler BL, Hughson FM.** 2011. A strategy for antagonizing quorum sensing. Mol Cell **42:**199–209. http://dx.doi.org/10.1016/j.molcel.2011.04.003.
12. **Kim T, Duong T, Wu CA, Choi J, Lan N, Kang SW, Lokanath NK, Shin D, Hwang HY, Kim KK.** 2014. Structural insights into the molecular mechanism of *Escherichia coli* SdiA, a quorum-sensing receptor. Acta Crystallogr D Biol Crystallogr **70:**694–707. http://dx.doi.org/10.1107/S1399004713032355.
13. **Bottomley MJ, Muraglia E, Bazzo R, Carfi A.** 2007. Molecular insights into quorum sensing in the human pathogen *Pseudomonas aeruginosa* from the structure of the virulence regulator LasR bound to its autoinducer. J Biol Chem **282:**13592–13600. http://dx.doi.org/10.1074/jbc.M700556200.
14. **Yao Y, Martinez-Yamout MA, Dickerson TJ, Brogan AP, Wright PE, Dyson HJ.** 2006. Structure of the *Escherichia coli* quorum sensing protein SdiA: activation of the folding switch by acyl homoserine lactones. J Mol Biol **355:**262–273. http://dx.doi.org/10.1016/j.jmb.2005.10.041.
15. **Zhu J, Winans SC.** 1999. Autoinducer binding by the quorum-sensing regulator TraR increases affinity for target promoters in vitro and decreases TraR turnover rates in whole cells. Proc Natl Acad Sci U S A **96:**4832–4837. http://dx.doi.org/10.1073/pnas.96.9.4832.
16. **Zhu J, Winans SC.** 2001. The quorum-sensing transcriptional regulator TraR requires its cognate signaling ligand for protein folding, protease resistance, and dimerization. Proc Natl Acad Sci U S A **98:**1507–1512. http://dx.doi.org/10.1073/pnas.98.4.1507.
17. **Michael B, Smith JN, Swift S, Heffron F, Ahmer BM.** 2001. SdiA of *Salmonella enterica* is a LuxR homolog that detects mixed microbial communities. J Bacteriol **183:**5733–5742. http://dx.doi.org/10.1128/JB.183.19.5733-5742.2001.
18. **Yamamoto K, Yata K, Fujita N, Ishihama A.** 2001. Novel mode of transcription regulation by SdiA, an *Escherichia coli* homologue of the quorum-sensing regulator. Mol Microbiol **41:**1187–1198. http://dx.doi.org/10.1046/j.1365-2958.2001.02585.x.
19. **Mellies JL, Barron AM, Carmona AM.** 2007. Enteropathogenic and enterohemorrhagic *Escherichia coli* virulence gene regulation. Infect Immun **75:**4199–4210. http://dx.doi.org/10.1128/IAI.01927-06.
20. **Sheng H, Lim JY, Knecht HJ, Li J, Hovde CJ.** 2006. Role of *Escherichia coli* O157:H7 virulence factors in colonization at the bovine terminal rectal mucosa. Infect Immun **74:**4685–4693. http://dx.doi.org/10.1128/IAI.00406-06.
21. **Brameyer S, Kresovic D, Bode HB, Heermann R.** 2015. Dialkylresorcinols as bacterial signaling molecules. Proc Natl Acad Sci U S A **112:**572–577. http://dx.doi.org/10.1073/pnas.1417685112.
22. **Brachmann AO, Brameyer S, Kresovic D, Hitkova I, Kopp Y, Manske C, Schubert K, Bode HB, Heermann R.** 2013. Pyrones as bacterial signaling molecules. Nat Chem Biol **9:**573–578. http://dx.doi.org/10.1038/nchembio.1295.
23. **Tsai CS, Winans SC.** 2011. The quorum-hindered transcription factor YenR of *Yersinia enterocolitica* inhibits pheromone production and promotes motility via a small non-coding RNA. Mol Microbiol **80:**556–571. http://dx.doi.org/10.1111/j.1365-2958.2011.07595.x.
24. **Alvarez HM, Steinbüchel A.** 2002. Triacylglycerols in prokaryotic microorganisms. Appl Microbiol Biotechnol **60:**367–376. http://dx.doi.org/10.1007/s00253-002-1135-0.
25. **Liu Q, Siloto RM, Lehner R, Stone SJ, Weselake RJ.** 2012. Acyl-CoA: diacylglycerol acyltransferase: molecular biology, biochemistry and biotechnology. Prog Lipid Res **51:**350–377. http://dx.doi.org/10.1016/j.plipres.2012.06.001.
26. **Smith JN, Dyszel JL, Soares JA, Ellermeier CD, Altier C, Lawhon SD, Adams LG, Konjufca V, Curtiss R, III, Slauch JM, Ahmer BM.** 2008. SdiA, an N-acylhomoserine lactone receptor, becomes active during the transit of *Salmonella enterica* through the gastrointestinal tract of turtles. PLoS One **3:**e2826. http://dx.doi.org/10.1371/journal.pone.0002826.
27. **Sambrook JFE, Maniatis T.** 1989. Molecular cloning: a laboratory manual, 2nd ed. Cold Spring Harbor Laboratory Press, Cold Spring Harbor, NY.
28. **Uzzau S, Figueroa-Bossi N, Rubino S, Bossi L.** 2001. Epitope tagging of chromosomal genes in *Salmonella*. Proc Natl Acad Sci U S A **98:**15264–15269. http://dx.doi.org/10.1073/pnas.261348198.
29. **Datsenko KA, Wanner BL.** 2000. One-step inactivation of chromosomal genes in *Escherichia coli* K-12 using PCR products. Proc Natl Acad Sci U S A **97:**6640–6645. http://dx.doi.org/10.1073/pnas.120163297.
30. **Walters M, Sperandio V.** 2006. Autoinducer 3 and epinephrine signaling in the kinetics of locus of enterocyte effacement gene expression in enterohemorrhagic *Escherichia coli*. Infect Immun **74:**5445–5455. http://dx.doi.org/10.1128/IAI.00099-06.